Eur. J. Mech. B/Fluids, **18**, (1), 131-145, 1999

New insights on steady, non-linear flow in porous media

E. SKJETNE [a], J.L. AURIAULT [b]*

ABSTRACT. – We consider two problems of nonlinear flow in porous media: 1) a derivation of a cubic weak inertia correction of Darcy's law which is valid for any matrix anisotropy, and 2) a description of flow by the weak inertia equation for low Reynolds numbers and a Forchheimer equation for high Reynolds number laminar flow. Recent homogenization studies show that the weak inertia correction to Darcy's law is not a square term in velocity, as it is in the Forchheimer equation, but instead a cubic term in velocity. By imposing that the pressure loss is invariant under flow reversion, it has been shown that the weak inertia equation is valid even for anisotropic media. We show, by using the homogenization technique, that the weak inertia equation is valid for any anisotropic matrix symmetry without imposing a reversed flow symmetry. For the second problem, we reexamine published data. We find that the description 2) applies well. A spline may be applied in the crossover regime.© Elsevier, Paris.

1. Introduction

For sufficiently low pore Reynolds numbers R, the steady state flow of incompressible fluids through porous media is described by the celebrated Darcy's law. The velocity v is linearly related to the gradient of pressure

$$v_i = -\frac{K_{ij}}{\mu}\frac{\partial p}{\partial X_j}, \tag{1}$$

where $\mathbf{K}$ is the permeability tensor and μ is the viscosity. It is generally admitted that the upper limit of validity of Darcy's law is for Reynolds numbers (based on average velocity and grain size) between 1 and 10, depending on the geometry, see e.g. (Bear 1992).

As the Reynolds number increases, nonlinearities appear. They are due to inertia. Up to Reynolds numbers approximately 100, the flow regime remains laminar. This limit, as well as the upper limit of the linear laminar flow regime is rather fuzzy. It depends strongly on the pore geometry and the Reynolds number itself cannot be defined in a single way from the flow parameters. For higher Reynolds numbers, the flow becomes turbulent. The three flow regimes have been identified from experimental investigations, e.g. (Chauveteau and Thirriot, 1967; Dybbs and Edwards, 1984), and laminar flow has been studied numerically in (Barrère, 1990; Edwards *et al.*, 1990; Firdaouss and Guermond, 1995; Skjetne, Thovert and Adler, 1995; Skjetne, Hansen and Gudmundsson, 1995).

To describe the nonlinear flow in porous media, the deviation from Darcy's law is usually described by the so called Forchheimer equation. Forchheimer (1901), proposed that the high-velocity correction to Darcy's law was proportional to a power m of the velocity

$$-\frac{\partial p}{\partial X} = av + bv^m, \tag{2}$$

* Correspondence and reprints.

[a] Department of Petroleum Engineering, Stanford University, Stanford, CA 94305-2220, U.S.A. Present address: Åsgard Petek, Statoil, N-4035 Stavanger, Norway.

[b] Laboratoire "Sols, Solides, Structures", UJF, INPG, CNRS UMR 5521, BP 53X, 38041 Grenoble cedex, France.

0997-7546/99/01/© Elsevier, Paris

where m is close to 2. Forchheimer also proposed that the pressure loss could be described by a third order polynomial in velocity

$$-\frac{\partial p}{\partial X} = av + bv^2 + cv^3. \tag{3}$$

Based on a dimensional analysis of Muskat (1937), Green and Duwez (1951) and Cornell and Katz (1953) found that the coefficients of (2) with $m = 2$, can be separated in fluid and rock parameters, and it is the following equation which is today called the Forchheimers equation

$$-\frac{\partial p}{\partial X} = \frac{\mu}{K} v + \beta \rho v^2, \tag{4}$$

where β is a rock parameter termed the inertial resistance, β-factor, high-velocity flow coefficient, or non-Darcy flow coefficient.

The Forchheimer equation (4) is now the standard equation for describing high-velocity flow in petroleum engineering, and also low velocity flow in the sense that (4) reduces to Darcy's law for low velocities (Firoozabadi and Katz, 1979; Firoozabadi *et al.*, 1995). In chemical engineering, the Ergun equation (Ergun, 1952) has the same velocity dependence as the Forchheimer equation, and accounts also for some porosity dependence in the permeability and inertial resistance. Typically, high-velocity flow experiments are analyzed by constructing a so called Forchheimer or resistance plot, that is plotting the negative pressure gradient (for liquid flow) divided by rate versus rate, and estimating the permeability and inertial resistance from the best fitted straight line.

In contrast to the traditional analysis, numerous experiments and numerical studies show that the Forchheimer equation is not strictly valid and that the macroscopic description of the flow changes with Reynolds number. Chauveteau and Thirriot (1967) classified flow regimes with different macroscopic descriptions, and made an important distinction between geometrically simple and complex media, each with a separate classification of flow regimes. To incorporate some recent progress in the understanding of the effect of weak inertia, Skjetne, Thovert and Adler (1995) reclassified the system of Chauveteau and Thirriot (1967). For geometrically simple media (such as bended tubes) the flow regimes are: 1) Darcy, 2) Weak inertia 3) Strong inertia, and 4) Turbulence. For geometrically complex media the flow regimes are: 1) Darcy, 2) Weak inertia, 3) Transition from Weak to Strong inertia, 4) Strong inertia, 5) Transition from Strong inertia to Turbulence, and 6) Turbulence.

Recent studies devoted to the effect of low, but not completely neglegible, Reynolds numbers (weak inertia, flow regime 2) on the macroscopic flow description show that the Forchheimer equation is not correct. It turns out often that the correction to Darcy's law is a cubic term in velocity given by

$$-\frac{\partial p}{\partial X} = \frac{\mu}{K} v + \frac{\gamma \rho^2}{\mu} v^3, \tag{5}$$

where γ is a rock dependent dimensionless parameter. This was first shown numerically on a periodic two-dimensional porous medium by Barrère (1990), and has later been confirmed by Firdaouss and Guermond (1995), Skjetne, Thovert and Adler (1995) and Skjetne, Hansen and Gudmundsson (1995). Earlier experimental data (Muskat, 1937; Chauveteau and Thirriot, 1965; Chauveteau and Thirriot, 1967; Fand *et al.*, 1987) are qualitatively in accordance with (5), but has not yet been reexamined.

The appearance of a cubic correction term was demonstrated in (Mei and Auriault, 1991), for homogeneous isotopic porous media or for one-dimensional flows. It was obtained from the pore scale description by assuming a periodic porous medium. The method of multiple scale expansions was used, and gave the macroscopic equivalent behaviour without any prerequisite at the macroscopic scale. The Reynolds number R was assumed

to be low, $R = O(\varepsilon^{1/2})$, where ε is the small scale separation parameter, $\varepsilon = l/L$. l and L are the characteristic lengths of the pores and the macroscopic flow, respectively.

By using the same method, different other cases with low R are investigated in (Wodie and Levy, 1991; Wodie, 1992); Rasoloarijaona, 1993; Rasoloarijaona and Auriault, 1994). A good survey of these theoretical results can be found in (Rasoloarijaona, 1993, p. 144–145), where non-polynomial models are also presented. The method of multiple scale expansions enables one to calculate the coefficients in (5). Rasoloarijaona (1993) and Rasoloarijaona and Auriault (1994) seized this opportunity to check relation (5) by fitting (5) to experimental channel flow data for $R<150$ and then comparing experimental and calculated coefficients.

Under the condition that the flow equation is invariable when reversing the flow direction, it is also demonstrated in (Firdaouss and Guermond, 1995) that (5) is valid for low Reynolds numbers, whatever the matrix anisotropy. The case of finite R is investigated in (Auriault, 1996) by using the theory of the representation of tensorial isotropic functions. When assuming that the nonlinear flow equation is a polynomial, it is shown that the cubic law (5) is valid for orthotropic or transverse isotropic media in the whole laminar flow regime. The numerical study (Firdaouss and Guermond, 1995) on particular geometries confirms that the cubic law is valid for a limited range of Reynolds numbers above unity. For a geometry similar to the converging-diverging channel in (Firdaouss and Guermond, 1995), it is shown experimentally that the flow is no longer invariable when reversing the flow direction when the Reynolds number is above about ten (Chauveteau and Thirriot, 1967).

Theoretically, the weak inertia equation is likely to break down for Reynolds numbers of the order of unity. For Reynolds numbers of order unity, homogenization of the Navier-Stokes equations shows that the leading order flow problem becomes non-linear and the macroscopic flow equation becomes, in general, non-linear (Sanchez-Palencia, 1980; Auriault *et al.*, 1990). It is no reason to expect that Darcy's law is a part of the non-linear solution. Two consequences of this are 1) that the weak inertia equation is likely to break down for Reynolds numbers of order unity and 2) equations for strong inertia laminar flow formulated as extensions of Darcy's law, such as (2) with $a = \mu/K$ and the standard Forchheimer equation (4), are generally not valid.

Strong inertial flow (flow regime 4) in complex media is described by a modified Forchheimer equation (Muskat, 1937; Chauveteau and Thirriot, 1967; Fand *et al.*, 1987; Couland *et al.*, 1988; Skjetne, Thovert and Adler, 1995; Skjetne, Hansen and Gudmundsson, 1995)

$$-\frac{\partial p}{\partial X} = \frac{\mu}{K_{fh}} v + \beta \rho v^2, \tag{6}$$

where $K_{fh} \neq K$. Anisotropic media follow (6) with a direction dependent β (Barak and Bear, 1981).

In contrast, strong inertial flow (flow regime 3) in simple media is not described by (6). Instead, it has been suggested to use (2) with $1 < m < 2$ (Chauveteau and Thirriot, 1965), or simply a power law with $1 < m < 2$ (Chauveteau and Thirriot, 1967)

$$-\frac{\partial p}{\partial X} = b v^m. \tag{7}$$

The description of strong inertial flow lacks rigorous theoretical support. Flow in simple model media and a simple scaling of the pressure loss indicate that a power $m = 3/2$ is a result of ideal boundary layer flow (Chauveteau and Thirriot, 1965; Skjetne, Hansen and Gudmundsson, 1995).

Turbulent flow in simple (flow regime 4) and complex media (flow regime 6) is described by a modified Forchheimer equation (Chauveteau and Thirriot, 1967; Fand *et al.*; 1987)

$$-\frac{\partial p}{\partial X} = \frac{\mu}{K_{fh,t}} v + \beta_t \rho v^2, \tag{8}$$

where in general $K_{fh,t} \neq K_{fh}$ and $\beta_t \neq \beta$. For complex media, $K_{fh,t} \leq K_{fh}$ and $\beta_t \leq \beta$.

Some studies show a detailed picture of the different flow regimes (Chauveteau and Thirriot, 1967; Dybbs and Edwards, 1984; Skjetne, Thovert and Adler, 1995; Skjetne, Hansen and Gudmundsson, 1995). Chauveteau and Thirriot (1967) showed that in the transition regime between laminar and turbulent flow, the flow is laminar in some pores and turbulent in other pores. Dybbs and Edwards (1984) studied how velocity fields changed with Reynolds numbers for hexagonal cylinder packings, and observed boundary layers at the walls and also free boundary layers. For Reynolds numbers close to the onset of turbulence unsteady laminar oscillations were observed. Skjetne, Thovert and Adler (1995) and Skjetne, Hansen and Gudmundsson (1995) studied numerically both low and high Reynolds number laminar flow through periodic porous media. For low Reynolds numbers, (5) described the flow data well, whereas for higher Reynolds numbers (6) described the data well. For intermediate Reynolds numbers, there was a crossover regime (flow regime 3) where none of the two equations applied well.

Regarding local effects of inertia in the Forchheimer flow regime, it was found in (Skjetne, Thovert and Adler, 1995; Skjetne, Hansen and Gudmundsson, 1995) that the fluid with high velocity was localized in narrow flow tubes, which were almost piecewise linear in open pores and changed direction after impinging into the pore walls. The macroscopically extra pressure loss was due to the combined effects of 1) increased wall friction at locations where a flow tube impinged and formed a boundary layer and 2) that the local Reynolds number in the flow tubes increased faster than the seepage velocity due to flow tube narrowing with increasing Reynolds numbers. The weak inertia flow regime is described by a transition from a wide spread diffusion dominated flow (Stokes equation) to inertia dominated flow tubes. The exotic effects of velocity "dip" and "core" flow observed experimentally by Dybbs and Edwards (1984) can be understood in terms of flow tube interaction (Skjetne, Thovert and Adler, 1995). Flow tubes can also be seen in (Chauveteau and Thirriot, 1967).

The aim of this paper is to bring some new insight into the modelling of the nonlinearities in the laminar flow regime. In Section 2, we study flow at low Reynolds numbers in the range $\varepsilon^{1/2} \ll R \ll 1$. We show that the assumption of invariance under reverse flow as introduced in (Firdaouss and Guermond, 1995) is unnecessary. In that range, the weak inertia equation (5) is valid whatever the degree of anisotropy of the porous matrix. Experimental checkings of the nonlinear model are generally conducted on a wide range of the Reynolds number, that comprises the linear Darcy range, the nonlinear laminar range and sometimes the nonlinear turbulent range. Since the laws describing the flow even in the laminar flow regimes may be dissimilar, analysis with only one law for all the data may be doubtful. In Section 3 we reexamine different flow data: experimental data by (Rasoloarijaona and Auriault, 1994), (Chauveteau and Thirriot, 1967) and (Fand *et al.*, 1987); numerical data by (Couland *et al.*, 1986) and (Skjetne, Thovert and Adler, 1995; Skjetne, Hansen and Gudmundsson, 1995). We distinguish the weak inertia from the Forchheimer flow regime, and also consider the shape of the crossover in a resistance plot.

2. Flow with low Reynolds numbers

We consider a periodic porous matrix of period Ω saturated by an incompressible fluid. The pores occupy Ω_p and the pore surface is denoted Γ. The flow is laminar and steady. The fluid velocity V and the pressure P verify

$$\mu \frac{\partial^2 V_i}{\partial X_j \partial X_j} - \frac{\partial P}{\partial X_i} = \rho V_j \frac{\partial V_i}{\partial X_j}, \tag{9}$$

$$\frac{\partial V_i}{\partial X_i} = 0 \qquad \text{in} \quad \Omega_p, \tag{10}$$

$$V_i = 0 \qquad \text{on} \quad \Gamma. \tag{11}$$

V_i and $\partial P/\partial X_i$ are Ω-periodic. μ is the viscosity and ρ is the fluid density. The above set is put in dimensionless form by introducing the dimensionless space variable $y_i = X_i/l$ and adequate characteristic quantities, e.g. balance between macroscopic pressure gradient and microscopic viscous force leads to $p = (P/L)/(\mu V/l^2)$ (Rasoloarijaona and Auriault, 1994)

$$\frac{\partial^2 v_i}{\partial y_j \partial y_j} - \varepsilon^{-1} \frac{\partial p}{\partial y_i} = R v_j \frac{\partial v_i}{\partial y_j}, \tag{12}$$

$$\frac{\partial v_i}{\partial v_i} = 0 \qquad \text{in} \quad \Omega_p, \tag{13}$$

$$v_i = 0 \qquad \text{on} \quad \Gamma. \tag{14}$$

In equation (12) we have assumed $\varepsilon \ll R \ll \varepsilon^{-1}$. Due to the two characteristic lengths l and L each quantity depends on the two dimensionless space variables $y_i = X_i/l$ and $x_i = X_i/l$. Then, by following the multiple scale expansion technique (Sanchez-Palencia, 1980), the velocity $\mathbf{v}$ and the pressure fluctuation p are looked for in the form of asymptotic expansions of powers of ε

$$\mathbf{v} = \mathbf{v}^{(0)}(\mathbf{x}, \mathbf{y}) + \varepsilon \mathbf{v}^{(1)}(\mathbf{x}, \mathbf{y}) + \varepsilon^2 \mathbf{v}^{(2)}(\mathbf{x}, \mathbf{y}) + \cdots \tag{15}$$

$$p = p^{(0)}(\mathbf{x}, \mathbf{y}) + \varepsilon p^{(1)}(\mathbf{x}, \mathbf{y}) + \varepsilon^2 p^{(2)}(\mathbf{x}, \mathbf{y}) + \cdots \tag{16}$$

Introducing these expansions in (12)–(14) gives by identification of the like powers of ε successive boundary value problems to be investigated. The first order approximation of the pressure verifies

$$\frac{\partial p^{(0)}}{\delta y_i} = 0, \qquad p^{(0)} = p^{(0)}(\mathbf{x}). \tag{17}$$

The first order approximation of the velocity $\mathbf{v}^{(0)}$ and the second order approximation of the pressure $p^{(1)}$ are determined by the following set

$$\frac{\partial^2 v_i^{(0)}}{\partial y_j \partial y_j} - J_i - \frac{\partial p^{(1)}}{\partial y_i} = R v_j^{(0)} \frac{\partial v_i^{(0)}}{\partial y_j}, \tag{18}$$

$$\frac{\partial v_i^{(0)}}{\partial v_i} = 0 \qquad \text{in} \quad \Omega_p, \tag{19}$$

$$v_i^{(0)} = 0 \qquad \text{on} \quad \Gamma. \tag{20}$$

$\mathbf{v}^{(0)}$ and $p^{(1)}$ are Ω-periodic. $J_i = \partial p^{(0)}/\partial x_i$ is the macroscopic pressure gradient that causes the flow. For an experiment, either $\mathbf{J}$ or the average velocity should be specified. To investigate this boundary value problem, it is convenient to introduce the space $\mathcal{W}$ of periodic divergence free vectors, defined on Ω_p, nul on Γ, with the scalar product:

$$(\mathbf{u}, \mathbf{v})_{\mathcal{W}} = \int_{\Omega_p} \frac{\partial u_i}{\partial y_j} \frac{\partial v_i}{\partial y_j} \, \mathrm{d}y, \tag{21}$$

which satisfies the following symmetry

$$(\mathbf{u}, \mathbf{v})_{\mathcal{W}} = (\mathbf{v}, \mathbf{u})_{\mathcal{W}}. \tag{22}$$

Now, multiply the two numbers of (18) by $\mathbf{u} \in \mathcal{W}$ and integrate over Ω_p. By using integration by parts, the divergence theorem, the boundary condition on Γ and periodicity, it becomes:

$$\forall\, \mathbf{u} \in \mathcal{W}, \qquad (\mathbf{u}, \mathbf{v}^{(0)})_{\mathcal{W}} = -R\, b(\mathbf{v}^{(0)}, \mathbf{v}^{(0)}, \mathbf{u}) - (\mathbf{u}, \mathbf{J})_{\mathrm{L}^2}, \tag{23}$$

where the trilinear form b is defined as

$$b(\mathbf{u}, \mathbf{v}, \mathbf{w}) = \int_{\Omega_p} u_i \frac{\partial v_j}{\partial y_i} w_j \, \mathrm{d}y. \tag{24}$$

This formulation is equivalent to the set of (18)–(20). We now consider low Reynolds numbers. As in Firdaouss and Guermond (1995), we look for $\mathbf{v}^{(0)}$ in the form of the expansion

$$\mathbf{v}^{(0)} = \mathbf{v}^0 + R\,\mathbf{v}^1 + R^2\,\mathbf{v}^2 + \cdots \tag{25}$$

This development is valid up to the term $R^n\,\mathbf{v}^n$ on the condition that

$$\varepsilon^{1/n} \ll R \ll 1 \tag{26}$$

Introducing the above expansion in the formulation (23) and identifying like powers of R give successively

$$\forall\, \mathbf{u} \in \mathcal{W}, \qquad (\mathbf{u}, \mathbf{v}^0)_{\mathcal{W}} = -(\mathbf{u}, \mathbf{J})_{\mathrm{L}^2}, \tag{27}$$

$$\forall\, \mathbf{u} \in \mathcal{W}, \qquad (\mathbf{u}, \mathbf{v}^1)_{\mathcal{W}} = -b(\mathbf{v}^0, \mathbf{v}^0, \mathbf{u}) \tag{28}$$

$$\forall\, \mathbf{u} \in \mathcal{W}, \qquad (\mathbf{u}, \mathbf{v}^2)_{\mathcal{W}} = -b(\mathbf{v}^1, \mathbf{v}^0, \mathbf{u}) - b(\mathbf{v}^0, \mathbf{v}^1, \mathbf{u}). \tag{29}$$

As expected, the first approximation (27) is the Darcy linear formulation. It gives

$$v_i^0 = -k_{ij} J_j, \tag{30}$$

which by averaging yields Darcy's law

$$\langle v_i^0 \rangle = -K_{ij} J_j, \qquad \mathbf{K} = \langle \mathbf{k} \rangle = \frac{1}{\Omega} \int_{\Omega_p} \mathbf{k} \mathrm{d}y. \tag{31}$$

The vector $\mathbf{k}_{.j}$ is solution of the following variational form

$$\forall\, \mathbf{u} \in \mathcal{W}, \qquad (\mathbf{u}, \mathbf{k}_{.j})_{\mathcal{W}} = (\mathbf{u}, \mathbf{I}_{.j})_{\mathrm{L}^2}, \tag{32}$$

where $\mathbf{I}$ is the identity matrix.

From (28) we see that $\mathbf{v}^1$ is a linear homogeneous vectorial function of the $J_i J_j$'s

$$v_i^1 = -a_{ijk} J_j J_k, \tag{33}$$

which by averaging yields the first velocity corrector

$$\langle v_i^1 \rangle = -A_{ijk} J_j J_k, \qquad \mathbf{A} = \langle \mathbf{a} \rangle = \frac{1}{\Omega} \int_{\Omega_p} \mathbf{a} \mathrm{d}y. \tag{34}$$

By construction we have the symmetry

$$A_{ijk} = A_{ikj} \tag{35}$$

The vector $\mathbf{a}_{.jk}$ is solution of the following variational form

$$\forall\, \mathbf{u} \in \mathcal{W}, \qquad (\mathbf{u}, \mathbf{a}_{.jk})_{\mathcal{W}} = \int_{\Omega_p} u_i \frac{\partial k_{ik}}{\partial y_m} k_{mj} \, \mathrm{d}y. \tag{36}$$

To study $\mathbf{v}^1$, we firstly demonstrate that $\mathbf{A}$ is antisymmetric with respect to its first and third indices. We put $\mathbf{u} = \mathbf{a}_{.pq}$ in (32) to obtain

$$(\mathbf{a}_{.pq}, \mathbf{k}_{.j})_{\mathcal{W}} = \Omega \langle a_{jpq} \rangle = \Omega A_{jpq}. \tag{37}$$

We now put $\mathbf{u} = \mathbf{k}_{.j}$ in (36) written for $\mathbf{a}_{.pq}$

$$(\mathbf{a}_{.pq}, \mathbf{k}_{.j})_{\mathcal{W}} = \int_{\Omega_p} k_{ij} \frac{\partial k_{iq}}{\partial y_m} k_{mp} \, \mathrm{d}y. \tag{38}$$

We transform the right hand member of the above equation by using the divergence free character of $\mathbf{k}_{.j}$, the adherence condition, periodicity, and finally (38) and (37)

$$\begin{aligned} \int_{\Omega_p} k_{ij} \frac{\partial k_{iq}}{\partial y_m} k_{mp} \, \mathrm{d}y &= \int_{\Omega_p} \frac{\partial}{\partial y_m} (k_{mp} k_{iq} k_{ij}) \, \mathrm{d}y - \int_{\Omega_p} k_{mp} \frac{\partial k_{ij}}{\partial y_m} k_{iq} \, \mathrm{d}y \\ &= - \int_{\Omega_p} k_{mp} \frac{\partial k_{ij}}{\partial y_m} k_{iq} \, \mathrm{d}y = -(\mathbf{a}_{.pj}, \mathbf{k}_{.q})_{\mathcal{W}} = -\Omega A_{qpj}. \end{aligned} \tag{39}$$

Considering again (37) and (38), together with (39) yields the antisymmetry

$$A_{jpq} = -A_{qpj} \tag{40}$$

Remark that (39) shows that

$$\forall\, \mathbf{u}, \mathbf{v}, \mathbf{w} \in \mathcal{W}, \qquad b(\mathbf{u}, \mathbf{v}, \mathbf{w}) = -b(\mathbf{u}, \mathbf{w}, \mathbf{v}). \tag{41}$$

Now using (35) and (40) gives successively

$$A_{ijk} = A_{ikj} = -A_{jki} = -A_{jik} \tag{42}$$

and

$$A_{ijk} = -A_{jik} = A_{kij} = -A_{ikj} = -A_{ijk} \tag{43}$$

Therefore we obtain

$$A_{ijk} = 0, \qquad \langle \mathbf{v}^1 \rangle = 0. \tag{44}$$

The first correction to Darcy's law cancels out.

To study $\mathbf{v}^2$, we put $\mathbf{u} = \mathbf{v}^2$ in (27) and $\mathbf{u} = \mathbf{v}^0$ in (29), and get

$$(\mathbf{v}^2, \mathbf{J})_{\mathrm{L}^2} = -(\mathbf{v}^2, \mathbf{v}^0)_{\mathcal{W}} = b(\mathbf{v}^1, \mathbf{v}^0, \mathbf{v}^0) + b(\mathbf{v}^0, \mathbf{v}^1, \mathbf{v}^0). \tag{45}$$

From (41), the first term in the right hand member cancels out, and (45) reduces to

$$(\mathbf{v}^2, \mathbf{J})_{\mathrm{L}^2} = b(\mathbf{v}^0, \mathbf{v}^1, \mathbf{v}^0) = -b(\mathbf{v}^0, \mathbf{v}^0, \mathbf{v}^1) = (\mathbf{v}^1, \mathbf{v}^1)_{\mathcal{W}} \geq 0, \tag{46}$$

where we have used (41) and the formulation (28) with $\mathbf{u} = \mathbf{v}^1$.

The case $(\mathbf{v}^1, \mathbf{v}^1)_{\mathcal{W}} = 0$ yields $\partial v_j^1 / \partial y_i = 0$ in Ω_p. The adherence condition (14) then imposes $\mathbf{v}^1 = 0$. Considering again formulation (28), we then have

$$\forall\, \mathbf{u} \in \mathcal{W}, \qquad b(\mathbf{v}^0, \mathbf{v}^0, \mathbf{u}) = 0. \tag{47}$$

That gives

$$v_j^{(0)} \frac{\partial v_i^{(0)}}{\partial y_i} = 0. \tag{48}$$

This condition is checked in cylindrical pores, where the velocity is orthogonal to its gradient. It is easy to verify that in such a case $\mathbf{v}^p = 0$, $p \geq 1$. As expected for Reynolds numbers in the laminar range, nonlinearities cancel out and the linear Darcy regime is valid until turbulence.

However, for porous media with non cylindrical pores, the nonlinear term (48) does not cancel out everywhere in Ω_p. The left hand member in (46) is positive and

$$\langle \mathbf{v}^2 \rangle \neq 0. \tag{49}$$

Finally from (29), $\mathbf{v}^2$ and its average $\langle \mathbf{v}^2 \rangle$ appear as a linear vectorial function of the $J_i J_j J_k$'s. By using Darcy's law (31), the correction to Darcy's law is shown to be a cubic velocity term.

In conclusion it can be said that the correction to Darcy's law is a cubic velocity term, whatever the porous matrix anisotropy, when

$$\varepsilon^{1/2} \ll R \ll 1. \tag{50}$$

3. Data analysis and modeling of nonlinear flow

3.1. General

Our main goal is to show that the weak inertia equation fits the lower end of the so-called transition between the Darcy and Forchheimer regimes. Note that (5) was shown to hold, at least for $\varepsilon^{1/2} \ll R \ll 1$, and may in principle be valid for higher Reynolds numbers. We define the weak inertia and Forchheimer flow regimes as the range of Reynolds numbers (based on seepage velocity) where the respective equations match well the data. Non-linear effects are more clearly visualized in a Forchheimer plot than in a Darcy plot, so we display the results in Forchheimer plots.

We would also like to describe the crossover between the weak inertia and Forchheimer regimes. Initially, we tried a weighted average of the two models, with weights $0.5\,(1 \pm \tanh((v - v_{cr})/v_{wi}))$, where v_{cr} and v_{wi} are center and width of the crossover. This worked well for some data sets, but resulted in a hump at about v_{cr} for other data sets. Instead of using an interpolation, we have used a spline $(c_0 + c_1 v + c_2 v^2 + c_3 v^3)$ in a Forchheimer plot, which is determined by the values and derivatives of the weak inertia and Forchheimer equations at their respective endpoints.

Regarding model determination, we have minimized absolute and relative (square) errors. Which one to use depends on the errors of $-dp/dx$ and v. If the errors in $-dp/dx$ are of constant relative size, one should minimize relative errors. Minimizing absolute errors in $-dp/dx$ puts relatively more weight on the high velocity regime, so even if a model could fit the trend of the data in the low velocity regime, it may be forced to neglect it by fitting marginally better for higher velocities. Minimizing relative errors will honor more the trend of the low velocity data, but may not take properly into account the errors. We use absolute errors for the weak inertia regime and relative errors for the Forchheimer regime. This modeling fitted well the trend of the data.

3.2. Experiment: Rasoloarijaona and Auriault (1994)

The data of Rasoloarijaona and Auriault (1994) are for laminar flow ($R < 150$) through a tortuous channel consisting of 100 periods. The flow is driven by the difference in water level of a tank at inlet and outlet. We use the following notation:

$$v\,(i) = \langle v \rangle, \qquad G\,(i) = -\frac{p_1 - p_2}{L} \quad \text{for data point } i, \qquad i \in 1, \ldots, 14, \tag{51}$$

where p_1 and p_2 are inlet and outlet pressures, respectively. There are a few questionable points regarding the data analysis in (Rasoloarijaona and Auriault, 1994): 1) The point ($\langle v \rangle = 0$, $-(dp/dx) = 0$) was used as a data in the fits. 2) The fits were conducted over the whole range of velocities. 3) Absolute errors were minimized in the fits (see Figure 1). Let us point out the consequences of these three points.

A discrepancy in the zero level of the two tanks was expected, so that

$$-(dp/dx)|_{\langle v \rangle = 0} = \alpha, \qquad \alpha \neq 0. \tag{52}$$

Consequently, the data point (0, 0) should be excluded. The range of Reynolds numbers is then from 20 to 150. By fitting polynomials to the whole range of data, it could not be distinguished between different flow regimes. Absolute and relative errors are shown in Figure 1 (upper). Absolute and relative errors are correlated for $v < 0.06$ m/s, and relative errors are as large as – 20 % for $v(1)$. Probably there is information in the data which the models do not honor. This results in poor fits for low velocities.

To find the right model, it is crucial to determine well the offset. Experimental versions of the weak inertia (5) and Forchheimer (6) equations are

$$G = \alpha + av + cv^3, \qquad a = \frac{\mu}{K}, \qquad c = \frac{\gamma \rho^2}{\mu}, \tag{53}$$

$$G = \alpha + a_{fh} v + bv^2, \qquad a_{fh} = \frac{\mu}{K_{fh}}, \qquad b = \beta \rho. \tag{54}$$

Assuming positive curvature of G, an estimated lower bound for α, found by linear extrapolation to $v = 0$, is $\widehat{\alpha}_1$ = 289 Pa/m. The offsets in Rasoloarijaona and Auriault (1994), *i.e.* $\widehat{\alpha}$ for models S. and C.1. in Table I, are

smaller than $\widehat{\alpha}_1$. A better estimate is found by fitting to $v < 0.06$ m/s. Results of (53) and (54), and the cubic equation are given by W.I.1., F.1 and C.2 in Table I. The parameters of C.2 are inconclusive. Since W.I.1 has the smallest relative errors, we will in the following use $\widehat{\alpha} = \widehat{\alpha}_2 = 371$ Pa/m with $\widehat{\sigma}(\widehat{\alpha}_2) = 25$ Pa/m, where $\widehat{\sigma}$ is the estimated error. Fitting a cubic equation with a fixed $\widehat{\alpha}_2$ (C.3) gave $b = 0$, and supports our choice of $\widehat{\alpha}_2$. Corrected pressure losses G_c can be written $G_c = G(i) - \widehat{\alpha}$. Corrected data and the fits of Rasoloarijaona and Auriault (1994) are shown in Figure 1 (lower). The fits approach minus infinite as $v \to 0$ due to offset mismatch. Model fit results are tabulated in Table I. Parameters without a "$\pm$", except S. and C.1, are fixed.

TABLE I. – Fitted parameters. Models: W.I. = Weak Inertia, F. = Forchheimer, S. = Square, C. = Cubic. Parameters without a "$\pm$", except S. and C.1, are fixed. Fitted range $v < 0.06$ m/s: W.I.1, W.I.2, F.1, C.2 and C.3. Fitted range $v > 0.06$ m/s: F.2. Fitted range all data: W.I.3, F.3, S., and C.1. From Rasoloarijaona and Auriault (1994): S. and C.1.

Model	$\widehat{\alpha}$ [Pa/m]	a [Pa s/m^2]	a_{fh} [Pa s/m^2]	b [Pa s^2/m^3]	c [Pa s^3/m^4]
W.I.1	371 $\pm$ 6.7 %	1.75 10^4 $\pm$ 6.9 %			2.36 10^6 $\pm$ 13 %
W.I.2	371	1.755 10^4 $\pm$ 1.1 %			2.36 10^6 $\pm$ 5.0 %
W.I.3	371	1.855 10^4 $\pm$ 2.6 %			1.954 10^6 $\pm$ 4.0 %
F.1	456 $\pm$ 9.2 %		9.1 10^3 $\pm$ 30 %	2.5 10^5 $\pm$ 16 %	
F.2	371		8.4 10^3 $\pm$ 17 %	3.08 10^5 $\pm$ 4.9 %	
F.3	371		1.129 10^4 $\pm$ 6.5 %	2.74 10^5 $\pm$ 4.4 %	
S.	221		1.19 10^4	2.914 10^5	
C.1	59	2.76 10^4		- 1.574 10^3	1.43 10^6
C.2	290 $\pm$ 79 %	2.6 10^4 $\pm$ 95 %		- 2.5 10^5 $\pm$ 272 %	4.7 10^6 $\pm$ 134 %
C.3	371	1.75 10^4 $\pm$ 6.2 %		0 $\pm$ 6.6 10^4	2.35 10^6 $\pm$ 40 %

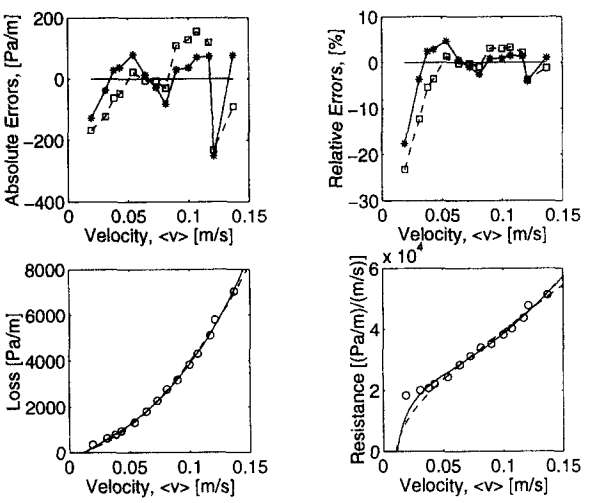

Fig. 1. – Flow data (circles) and fits of a square equation $G = \widehat{\alpha} + av + bv^2$ (dashed line and squares) and a cubic equation $G = \widehat{\alpha} + av + bv^2 + cv^3$ (solid line and stars) of Rasoloarijaona and Auriault (1994). Parameter values are given in Table I by model S. (square) and C.1 (cubic). (Upper left) Absolute errors and (upper right) relative errors of the fits. (Lower left) Darcy and (lower right) Forchheimer plots of data and fits corrected by $\widehat{\alpha}_2$.

Figure 2 shows (53) fitted in 0–0.06 m/s (dashed dotted line) and (54) fitted in 0.06–0.14 m/s (dashed line), with parameters given by W.I.2 and F.2 in Table I. The equations match the data well inside their respective ranges. From the Reynolds number range given in (Rasoloarijaona and Auriault, 1994), the weak inertia regime extends up to about $R = 50$. W.I.2 have parameters similar to W.I.1. Our fits gave $a_{fh} < a$, with

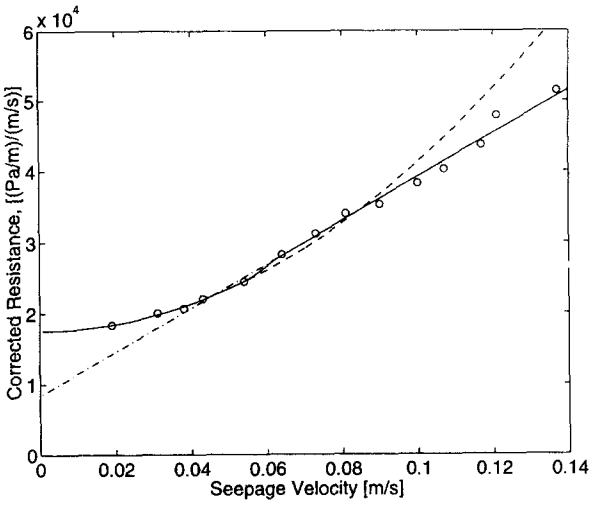

Fig. 2. – Forchheimer plot with corrected ($\widehat{\alpha}_2$) data of Rasoloarijaona and Auriault (1994) and fits of the weak inertia equation for $v < 0.06$ m/s (dashed line) and the Forchheimer equation for $v > 0.06$ m/s (dashed dotted line). The two fits are plotted in their respective ranges and connected by a spline in the crossover region (slid line).

a relative difference – 77 %. Thus, interpreting K_{fh} as K, may lead to large errors. To check the conclusion of Rasoloarijaona and Auriault (1994), we fitted (53) and (54), W.I.3 and F.3, to the whole range of data. These models did not fit well. The weak inertia equation has systematic errors: over for low velocities, under for intermediate velocities and over for high velocities. For the Forchheimer equation, the trend was the opposite.

3.3. Experiment: Chauveteau and Thirriot (1967)

Chauveteau and Thirriot (1967) measured gravity driven flow through a medium of isolated 2D grains of mean diameter d with hydraulic diameters equal to a 3D unconsolidated sand. For $R = 80$ (based on v and d), there was turbulence in one pore. A Forchheimer plot with scaled axes was constructed from a dimensionless friction factor $\lambda = -2\,(dh/dx)\,gd/v^2$, where dh/dx is the slope, and g is the acceleration of gravity: λR versus R. For simplicity, we do not rename a, a_{fh}, b, c in models with flow data proportional to G and v. Similarly, quantities proportional to G/v are labeled resistance. In Figure 3 the two models with parameters given in Table II follow the data well in their respective fitting ranges and poorly outside. For $R = 8.82$, the weak inertia loss it is only 4.4 % of the Darcy pressure loss and may explain the noise in the data.

3.4. Experiment: Fand et al. (1987)

Fand *et al.* (1987) measured flow of water through random packings of spheres for $0.18 \leq R \leq 408$. In Figure 4 we show the data $Gd/(\mu v)$ in [1/m] versus R up to the transition to turbulence $R < 80$ for spheres of diameter $d = 3.072$ mm, and fitted weak inertia and Forchheimer models with parameters given in Table II. The weak inertia model fits well. A tiny break in the Forchheimer slope at about $R = 40$ results in a fit slightly above the data for $R < 15$.

3.5. Simulation: Couland et al. (1986)

In Figure 5 we show the numerical data and fits to the resistance data of Couland *et al.* (1986), with parameters given in Table II, for flow with average entry velocity V_0 through a bank of cylinders with diameter d. The

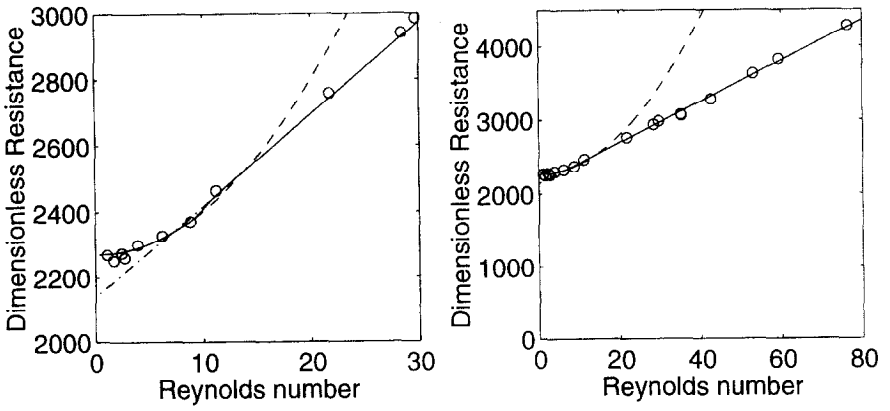

Fig. 3. – Data of Chauveteau and Thirriot (1967) with fits to the weak inertia and Forchheimer equations. (Right) the whole range of laminar flow and (left) data for low Reynolds numbers. Notations as in Figure 2.

TABLE II. – Parameters for data: (A) Chauveteau and Thirriot (1967) and (B) Fand *et al.* (1987), and (C) Couland *et al.* (1986). The parameters of model (A) and (C) are dimensionless. The parameters for model (B) are in [1/m].

Data	a	a_{fh}	b	c
A	2271 ± 0.30 %	2140 ± 1.09 %	27.7 ± 2.22 %	1.32 ± 8.67 %
B	$5.392\ 10^5$ ± 0.078 %	$5.093\ 10^5$ ± 0.35 %	$8.52\ 10^3$ ± 0.63 %	529.6 ± 2.6 %
C	89.17 ± 0.014 %	80.95 ± 0.079 %	1.263 ± 0.24 %	$5.02\ 10^{-2}$ ± 0.30 %

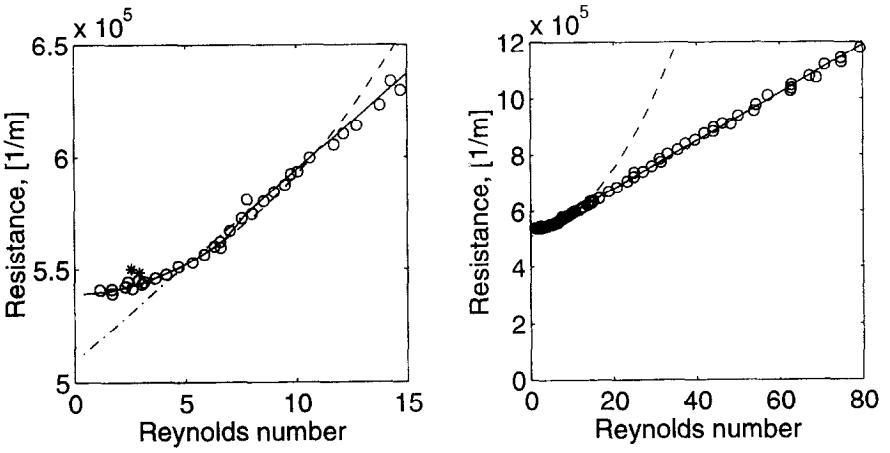

Fig. 4. – Data of Fand *et al.* (1987) with fits to the weak inertia and Forchheimer equations. (Right) the whole range of laminar flow, and (left) data for low Reynolds numbers. (Stars) two outlayer points which we excluded. A spline is drawn in the crossover regime $6.57 < R < 8$. Notations as in Figure 2.

dimensionless resistance is: $-\Delta p/(\rho V_0^2)\,(d/L)\,R$, where $-\Delta p$ is the pressure loss over the length L of the model. A spline is used in the crossover regime $10.2 < R < 13.1$. These data were also discussed in (Couland *et al.*, 1988). Both models fit very well.

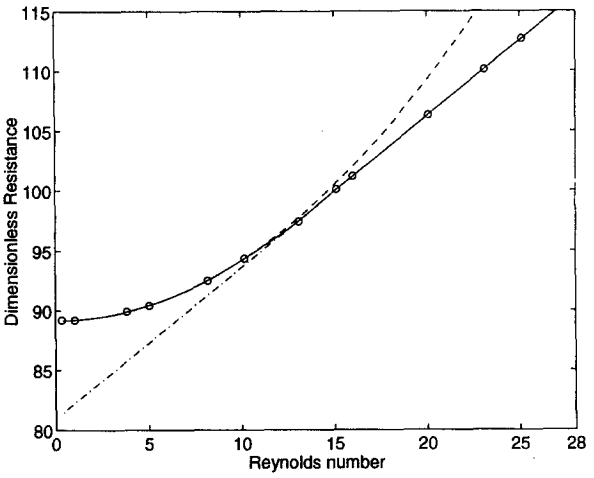

Fig. 5. – Data from Couland *et al.* (1986) with fits to the weak inertia and Forchheimer equations. A spline is drawn in the crossover regime $10.2 < R < 13.1$. Notations as in Figure 2.

3.6. Simulations: Skjetne, Hansen and Gudmundsson (1995) and Skjetne, Thovert and Adler (1995)

Figure 6 shows the numerical data for flow through a 2D self-affine rough fracture (Skjetne, Hansen and Gudmundsson, 1995), a cubic packing of spheres, with main flow in the (1,1,0)-direction (non-staggered), and a 3D reconstructed sandstone with porosity of 0.2 (Skjetne, Thovert and Adler, 1995). The fracture and sphere packing followed very well the weak inertia equation for flow velocities. Note the steep transition and strong resistance for the sandstone.

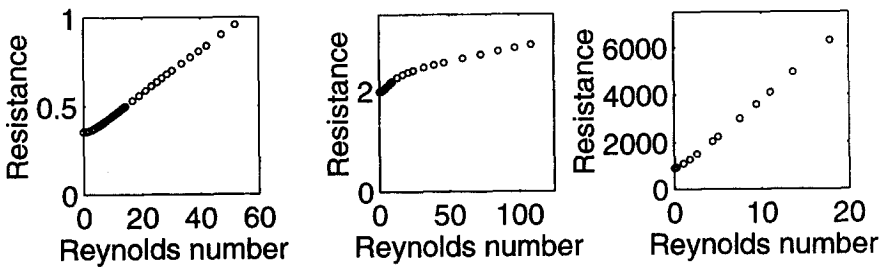

Fig. 6. – Forchheimer plots: (left) self-affine rough 2D fracture (Skjetne, Hansen and Gudmundsson, 1995), (middle) straight through a cubic packing of spheres, and (right) reconstructed sandstone (Skjetne, Thovert and Adler, 1995). The resistance is dimensionless.

The sphere packing data changes curvature in the crossover regime. In this case it seems that the slope at the upper end of the weak inertia regime is much greater than the Forchheimer slope, and the crossover data are under both extrapolated slopes. Thus, a weighted average of the extrapolated functions will always tend to overestimate the resistance. This explains why the interpolation function discussed previously had a hump in the crossover regime. Data for flow through a bank of cylinders (Lee and Yang, 1997) and a tube with varying cross section (Chauveteau and Thirriot, 1965) show the same type of resistance curve as the sphere packing.

A classification of the different resistance shapes may be based on the size of the Forchheimer slope b relative to the slope $2cR_1$ at the upper end of the weak inertia regime R_1. We have these possibilities: i) $b \simeq 2cR_1$, ii) $b < 2cR_1$ and iii) $b > 2cR_1$, as shown schematically in Figure 7. The reexamined data are of type i), while the sphere packing is of type ii). Consolidated sandstones may be of type iii).

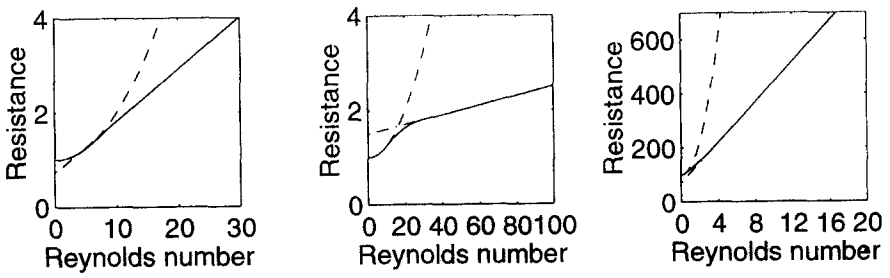

Fig. 7. – Examples of resistance curves: (left) $b \simeq 2cR_{\mathrm{I}}$ (i), (middle) $b < 2cR_{\mathrm{I}}$ (ii) and (right) $b > 2cR_{\mathrm{I}}$ (iii). The weak inertia (dashed line) and Forchheimer (dashed dotted line) equations are extrapolated. The equations are plotted in their respective ranges of validity and connected by a spline (solid line).

4. Conclusions

Theoretical analysis shows that the correction to Darcy's law is a cubic velocity term, whatever the porous matrix anisotropy, when

$$\varepsilon^{1/2} \ll R \ll 1, \tag{55}$$

i.e. for weak inertia flow. Reexamination of experimental and numerical flow data shows that the weak inertia and Forchheimer flow regimes can be distinguished. The weak inertia regime extended to porous media Reynolds numbers well above unity. The shape of the resistance in a crossover from weak inertia to Forchheimer flow is highly dependent on geometry.

Acknowledgments. – Financial support for E.S. to this study was from the Research Council of Norway through the project "Non-Darcy flow applications in petroleum science and technology" (111241/431) of the PROPETRO program.

REFERENCES

AURIAULT J.-L., 1996, Ecoulement non linéaire d'un fluide en milieu poreux rigide, C. R. Acad. Sci. Paris, Series II b, **323**, 169–196.

AURIAULT J.-L., STRZELECKI T., BAUER J., HE S., 1990, Porous deformable media saturated by a very compressible fluid: quasi-statics, Eur. J. Mech. A/Solids 9, 373–392.

BARAK A. Z., BEAR J., 1981, Flow at high Reynolds numbers through anisotropic porous media, Adv. Water Resources 4, 54–66.

BARRÈRE, 1990, Modélisation des écoulements de Stokes et Navier-Stokes en milieu poreux, Doctoral thesis at Université de Bordeaux I.

BEAR J., 1992, Dynamics of Fluids in Porous Media, Elsevier.

CHAUVETEAU G., THIRRIOT C., 1965, Sur les pertes de charge en écoulement laminaire dans quelques géométries simple et dans le milieu poreux, IX Convegno di idraulica e costruzioni idrauliche, Trieste, p. III A 3.

CHAUVETEAU G., THIRRIOT C., 1967, Régimes d'écoulement en milieu poreux et limite de la loi de Darcy, La Houille Blanche 2, 141–148.

CORNELL D., KATZ L. D., 1953, Flow of gases through consolidated porous media, Ind. Eng. Chem. 45, 2145–2152.

COULAND O., MOREL P., CALTAGIRONE J. P., 1986, Effets non linéaires dans les écoulements en milieu poreux, C. R. Acad. Sci. Paris, série II, 302, 263–266.

COULAND O., MOREL P., CALTAGIRONE J. P., 1988, Numerical modelling of nonlinear effects in laminar flow through a porous medium, J. Fluid Mech. 190, 393–407.

DYBBS A., EDWARDS R. V., 1984, A new look at porous media fluid mechanics - Darcy to turbulent, in Fundamentals of Transport Phenomena in Porous Media, number 82 in NATO ASI E, Martinus Nijhoff Publishers, Dordrecht, pp. 201–256.

EDWARDS D. A., SHAPIRO M., BAR-YOSEPH P., SHAPIRA M., 1990, The influence of Reynolds number upon the apparant permeability of spatially periodic arrays of cylinders, Phys. Fluids A 2, 45–55.

ERGUN S., 1952, Fluid flow through packed columns, Chem. Eng. Prog. 48, 89–94.

FAND R. M., KIM B. Y. K., LAM A. C. C., PHAN R. T., 1987, Resistance to the flow of fluids through simple and complex porous media whose matrices are composed of randomly packed spheres, J. Eng. Fluids 109, 268–274.

FIRDAOUSS M., GUERMOND J., 1995, Sur l'homogénéisation des équations de Navier-Stokes à faible nombre de Reynolds, C. R. Acad. Sci. Paris, série I, 320, 245–251.

FIROOZABADI A., KATZ D. L., 1979, An analysis of high-velocity gas flow through porous media, Journal of Petroleum Technology, pp. 211–216.

FIROOZABADI A., THOMAS L. K., TODD B., 1995, High-velocity flow in porous media, SPE Reservoir Engineering, pp. 149–152.

FORCHHEIMER P., 1901, Wasserbewegung durch Boden, Zeitschrift des Vereines deutscher Ingenieure 45, 1782–1788.

GREEN L., DUWEZ P., 1951, Fluid flow through porous-metals, J. Appl. Mech. 18, 39–45.

LEE S. L., YANG J. H., 1997, Modeling of Darcy-Forchheimer drag for fluid flow across a bank of circular cylinders, Int. J. Heat Mass Transfer 40, 3149–3155.

MEI C. C., AURIAULT J.-L., 1991, The effect of weak inertia on flow through a porous medium, J. Fluid Mech. 222, 647–663.

MUSKAT M., 1937, The Flow of Homogeneous Fluids Through Porous Media, International Human Resources Development Corporation, Reprint 1982.

RASOLOARIJAONA M., 1993, Non linéarités de la loi de Darcy : étude théorique, numérique et expérimentale. Thesis report, Laboratoire Sols, Solides, Structures, Université Joseph Fourier, Grenoble.

RASOLOARIJAONA M., AURIAULT J.-L. (1994), Nonlinear seepage flow through a rigid porous medium, Eur. J. Mech. B/Fluids, 13, 177–195.

SANCHEZ-PALENCIA E., 1980, Non Homogeneous Media and Vibration Theory, Vol. 127, Springer, Lecture Notes in Physics.

SKJETNE E., HANSEN A., GUDMUNDSSON J. S., 1995, High-velocity flow in a rough fracture, In Dr. Ing. Thesis by Skjetne E., High-velocity flow in porous media; analytical, numerical and experimental studies, Department of Petroleum Engineering and Applied Geophysics, Norwegian University of Science and Technology, 83–124.

SKJETNE E., THOVERT J.-F., ADLER P. M., 1995, High-velocity flow in spatially periodic porous, In Dr. Ing. Thesis by Skjetne E., High velocity flow in porous media; analytical, numerical and experimental studies, Department of Petroleum Engineering and Applied Geophysics, Norwegian University of Science and Technology, 9–82.

WODIE J.-C., 1992, Contribution à l'étude des milieux poreux par la méthode de l'homogénéisation : filtration non-linéaire, milieux fissurés. Thesis report, Université Pierre et Marie Curie, Paris.

WODIE J.-C., LEVY T., 1991, Correction non linéaire de la loi de Darcy, C. R. Acad. Sci. Paris, Série II, 312, 157–161.

(Received 19 December 1996;
revised 1 October 1997;
accepted 4 June 1998.)